

論文 / 著書情報  
Article / Book Information

Title	High Integrity Metal / Organic Device Interfaces via Low Temperature Buffer Layer Assisted Metal Atom Nucleation
Authors	Masato Maitani
Citation	App. Phys. Lett., Vol. 96, ,
Pub. date	2010, 3
URL	<a href="http://scitation.aip.org/content/aip/journal/apl">http://scitation.aip.org/content/aip/journal/apl</a>
Copyright	Copyright (c) 2010 American Institute of Physics

# High integrity metal/organic device interfaces via low temperature buffer layer assisted metal atom nucleation

Masato M. Maitani,<sup>1</sup> David L. Allara,<sup>1,a)</sup> Douglas A. A. Ohlberg,<sup>2</sup> Zhiyong Li,<sup>2</sup> R. Stanley Williams,<sup>2</sup> and Duncan R. Stewart<sup>3,a)</sup>

<sup>1</sup>Department of Chemistry, The Pennsylvania State University, University Park, Pennsylvania 16802, USA

<sup>2</sup>Information and Quantum Systems Laboratory, Hewlett-Packard Laboratories, 1501 Page Mill Road, MS 1123, Palo Alto, California 94304, USA

<sup>3</sup>National Research Council of Canada, Ottawa, Ontario K1A 0R6, Canada

(Received 2 January 2010; accepted 8 March 2010; published online 29 April 2010)

The ability to generate sharp, high integrity metal/organic film interfaces is demonstrated by the use of a buffer layer of Xe condensate during the vapor deposition of Au atoms onto a  $\text{CH}_3(\text{CH}_2)_{11}\text{S}/\text{Au}\{111\}$  self-assembled monolayer (SAM), a normally highly permeable film for the metal atoms in spite of the high degree of molecular organization and ordering. Atomic force microscopy conductance and topographic imaging reveals the intervening buffer can result in complete elimination of typical electrically shorting metal filaments and metal atom penetration into the SAM over large area contacts. This deposition method provides a highly reproducible way to form high integrity top metal contacts for demanding applications such as molecular electronic devices. © 2010 American Institute of Physics. [doi:10.1063/1.3377044]

Top metal overlayers on organic surfaces play a key role as electrical contacts in many types of electronic devices based on organic films, ranging across polymers to self-assembled molecular monolayers (SAMs) but often prove troublesome to prepare with the necessary integrity for device performance. Although vapor deposition is conventional since it conveniently forms uniform, large area contacts for a variety of metals, it is well appreciated that inhomogeneous overlayers and interfaces often result to give unfavorable device characteristics,<sup>1–6</sup> especially notable in molecular electronic devices, prepared, for example, with SAMs or Langmuir–Blodgett films at the 1–3 nm thickness scale. Achieving high integrity, abrupt metal-organic interfaces has been a major challenge, emphasized by reports revealing structural and chemical complexities such as metal penetration into the organic layer, chemical degradation, or erratic, nonuniform cluster and filament generation in and on the organic film.<sup>3,5–12</sup> These problems clearly hamper technological and fundamental advances in molecular junctions.<sup>10,12,13</sup> In order to circumvent such difficulties different vapor deposition methods, ranging across different types of metals, have been proposed, including indirect (prescattered metal atoms) deposition,<sup>14</sup> interlayer insertion,<sup>15</sup> and cooled substrate deposition.<sup>16</sup> In spite of these studies, a highly general method that produces high quality top contact molecular junctions has yet to be developed.

Herein we report the highly general method of buffer layer assisted growth (BLAG) in which the substrate organic film is precovered with an overlayer of a condensed noble gas which then serves as a soft landing layer to quench the kinetic energies of subsequent vapor deposited metal atoms.<sup>17,18</sup> This two-step-process mediates direct chemical and physical interactions of the impinging atoms with the organic surface region thereby preventing penetration, reduc-

ing or eliminating chemical degradation in the case of reactive metals, and overall providing a highly uniform medium for nucleation and growth. As an initial demonstration we chose the system of Au, a highly inert metal free of chemical complications as well as a common contact for molecular conduction devices, vapor deposited onto a  $\text{CH}_3(\text{CH}_2)_{11}\text{S}/\text{Au}\{111\}$  SAM (C12 SAM), a simple, well studied monolayer which, similar to a variety of SAMs, exhibits a high propensity for metal atom penetration under vapor deposition at ambient temperatures in spite of a high degree of organization and ordering.<sup>3,6–11</sup> Metal atom penetration in these types of SAMs dominantly arises from a dynamic adsorbate fluctuation process (similar to a localized lattice phonon) in which molecular diameter scale channels through the SAM to the substrate are transiently opened at random points across the monolayer to provide penetration paths.<sup>7,19</sup> Since the penetration is observed to be very uniform the selection of inert Au atoms deposited on the thin C12 SAM layer (thickness  $\sim 1.4$  nm) provides a severe test of the ability of any deposition method to stop metal atom penetration. In this report, we show that BLAG depositions can reproducibly result in complete cessation of the undesired penetration behavior to provide large area, high integrity device contacts.

SAMs were prepared by immersing freshly cleaved, atomically flat template stripped Au (TS-Au) (Ref. 20) in a degassed ethanol solution of 0.1 mM dodecanethiol and thoroughly rinsing with pure solvent.<sup>21,22</sup> After loading onto a sample stage, the sample was placed under vacuum ( $2 \times 10^{-10}$  Torr) and cooled (LHe cryostage) to  $\sim 10$  K. Exposure for selected times to Xe gas ( $2 \times 10^{-6}$  Torr) produced the desired thickness Xe condensate layers.<sup>17</sup> Gold was deposited via an e-beam source at  $5.9 \text{ atoms min}^{-1} \text{ nm}^{-2}$  ( $0.1 \text{ nm mass average min}^{-1}$ , equivalent to a  $0.1 \text{ nm min}^{-1}$  growth of an ideal uniform Au overlayer) as monitored by a quartz crystal microbalance next to the sample. Subsequently the sample stage was slowly heated to 70–85 K, carefully keeping the chamber pressure  $< 5 \times 10^{-6}$  Torr in order to

<sup>a)</sup>Authors to whom correspondence should be addressed. Electronic addresses: dla3@psu.edu and duncan.stewart@nrc.gc.ca.

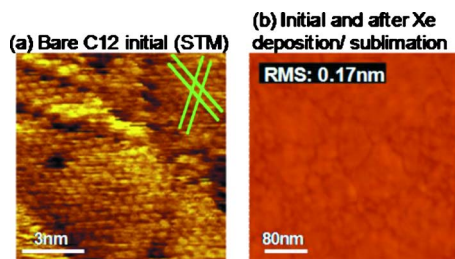


FIG. 1. (Color online) C12-SAM scanning probe images: (a) STM ( $10 \times 10$  nm) of the bare SAM; (b) t-AFM ( $0.4 \times 0.4$   $\mu\text{m}$ ;  $\pm 5$  nm Z-range) on the initial SAM. No changes in the t-AFM images were observed for samples after condensation and sublimation of Xe (150 ML), e.g., RMS roughnesses were equal at  $0.17 \pm 0.01$  nm. The STM images show the expected hexagonal lattice for the molecular packing (parallel green lines at  $60^\circ$  angles follow the lattice rows) along with the typical molecular domain and pit defects. (a) Bare C12 initial (STM) (b) initial and after Xe Deposition/sublimation.

avoid perturbation of the deposited Au by an abrupt Xe sublimation. After the pressure reached  $\sim 1 \times 10^{-9}$  Torr the sample temperature was increased to  $\sim 300$  K.

The scanning tunneling microscopy (STM) (RHK technologies, Troy, MI; Pt-Ir tip @ +1 V bias) image [Fig. 1(a)] of the initial bare C12 SAM surface in ultrahigh vacuum reveals the expected ( $\sqrt{3} \times \sqrt{3}$ ),  $R30^\circ$  crystalline lattice ( $a \sim 0.50$  nm) for a densely packed SAM with small fractions of typical intrinsic defects.<sup>1,11,20</sup> Tapping mode (t-AFM; Veeco Dimension 3100, Si cantilever) images in Fig. 1(b) show typical grain boundaries for the underlying TS-Au substrate and a highly uniform surface free of problematic features such as particles or other contamination. Conducting probe (cp-AFM; Veeco Multimode with CAFM mode, Pt-Ir cantilever @ 10 mV bias, 5 nN applied load) images (data not shown) show featureless, uniformly insulating surfaces up to the detection limit of our current amplifiers ( $\sim 0.5$  pA), typical for well organized alkanethiolate SAMs on polycrystalline Au substrates.<sup>14–16,23</sup> Further images after condensation and subsequent sublimation of 150 monatomic layers (MLs) of Xe condensate establish that the buffer layers themselves have no effects on the SAM topography or electrical properties.

Deposition of 472 Au atoms  $\text{nm}^{-2}$  (104 atoms per SAM molecule, equivalent to a 8 nm ideal uniform Au layer) on a C12 SAM at 10 K without BLAG treatment shows t-AFM features [Fig. 2(a)] similar to the initial SAM surface. This is typical of a “floating” SAM effect in which the deposited Au atoms effectively penetrate through the SAM to form a uniform underlayer at the Au-S interface, as previously reported (also see additional data in the supplementary material, Ref. 25).<sup>3,7–11,19</sup> In addition, the cp-AFM images reveal the presence of many scattered short-circuit filaments that typically arise at step edge or grain boundary defects.<sup>9</sup>

Changing to Au deposition at  $\sim 10$  K sample temperature does not stop metal atom penetration. The t-AFM images [Fig. 2(b)] for 472 Au atoms  $\text{nm}^{-2}$  (103 Au atoms per SAM molecule or equivalent to an 8.0 nm ideal uniform Au layer) show the SAM surfaces remain smooth ( $\sim 0.2$  nm), similar to the room temperature result. Cp-AFM, however, reveals significant numbers of scattered short-circuit points [Fig. 2(c)] which exhibit linear, Ohmic conductance behavior (data not shown) and thus can be attributed to metal filaments. These results are in agreement with reports that cryo-

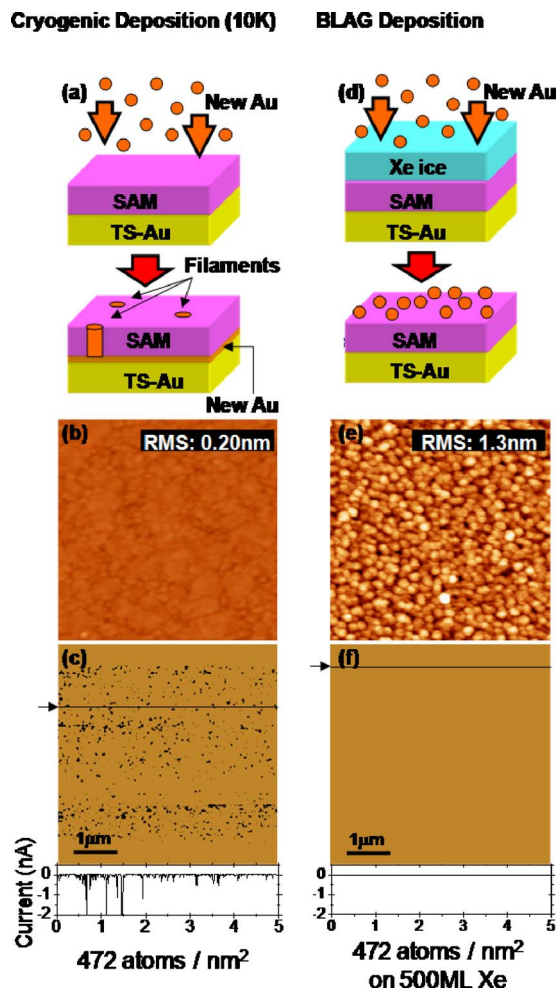


FIG. 2. (Color online) Results of Au deposition directly onto a SAM at 10 K (a) and under BLAG conditions with Xe ice (d). The corresponding t-AFM ( $0.4 \times 0.4$   $\mu\text{m}$ ) and cp-AFM ( $5 \times 5$   $\mu\text{m}$ ) images (Z ranges  $\pm 5$  nm and  $\pm 2$  nA for t- and cp- images, respectively) reshown in (b) and (c), respectively, for direct deposition and in (e) and (f), respectively, for BLAG deposition. Line scans (black lines across the cp-images) (bottom) show current spikes (some larger than the scale truncated at  $-2$  nA). Black spots in the cp-images indicate short-circuit filaments growing during Au deposition. Notice the fully insulating character in (f) which shows the striking absence of filament growth in the BLAG process. The corresponding morphology in (e) shows a uniform continuous sheet of  $\sim 7(\pm 1)$  nm Au clusters.

genic conditions alone do not provide high yields of metal-SAM-metal molecular junction devices.<sup>13,14</sup>

In contrast to the above results, Au deposition under selected BLAG conditions shows the ability to totally eliminate short-circuit filament formation, as seen in Fig. 2(f) for deposition of 472 Au atoms  $\text{nm}^{-2}$  on 500 ML of Xe which results in a fully insulating behavior over a  $25$   $\mu\text{m}^2$  area. Careful analysis of each of  $512 \times 512$  data spots within three different  $5.0 \times 5.0$   $\mu\text{m}^2$  scanning areas on the sample surface shows no measured currents higher than 50 pA, a remarkably low current for a large area Au overlayer, consistent with tunneling conduction (see below).

A number of different BLAG conditions were examined with representative results in Fig. 3, along with an ambient temperature control. The variation in the Au morphology with BLAG conditions is consistent with previous studies<sup>17,18,24</sup> and we note that the lowest conduction sample consists of a uniform sheet of  $\sim 7(\pm 1)$  nm Au clusters [Fig.



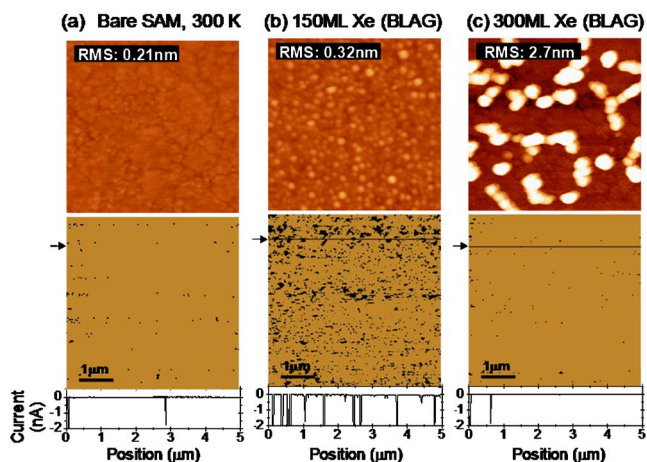


FIG. 3. (Color online) t-AFM ( $0.4 \times 0.4 \mu\text{m}$ ) and cp-AFM ( $5 \times 5 \mu\text{m}$ ) images of  $118 \text{ atoms/nm}^2$  deposited on C12 SAMs. (a) Room temperature (300 K); (b) with 150 ML Xe at 10 K (BLAG); and (c) with 300 ML Xe at 10 K (BLAG). Z ranges are  $\pm 5 \text{ nm}$  and  $\pm 2 \text{ nA}$  for t- and cp-images, respectively. Line scans (black lines across the cp-images; bottom) show the current spikes.

2(e); see also supplementary material, Ref. 25). Clearly, there is an optimum set of conditions for achieving fully insulating behavior.

In order to thoroughly probe the integrity of BLAG contacts over large areas, a BLAG deposition of  $1180 \text{ Au atoms nm}^{-2}$  (256 Au atoms per SAM molecule; equivalent 20 nm ideal thickness of uniform Au) at  $\sim 10 \text{ K}$  with a 1000 ML Xe buffer layer, was performed through a shadow mask to prepare an array of large area ( $\sim 50 \mu\text{m}^2$ ) Au/SAM/Au devices. The I-V responses, measured by cp-AFM on the Au top contact pads, show the dominant response is nonresonant tunneling (Fig. 4)<sup>13,15,23</sup> with average currents of  $\sim 1 \text{ nA } \mu\text{m}^{-2}$  or  $\sim 2 \times 10^{-16} \text{ A molecule}^{-1}$  [ $\sim 4.6 \times 10^6 \text{ C12 molecules } \mu\text{m}^{-2}$ , see Fig. 1(a)]. These currents are lower than ideal based on reported tunneling currents (at 0.2 V) of  $\sim 10^{-13} - 10^{-14} \text{ A molecule}^{-1}$  (Refs. 13, 15, and 23) but are fully consistent with a point probe contacting the Au overlayer, which is expected to have both imperfect contact with the underlying SAM molecules and

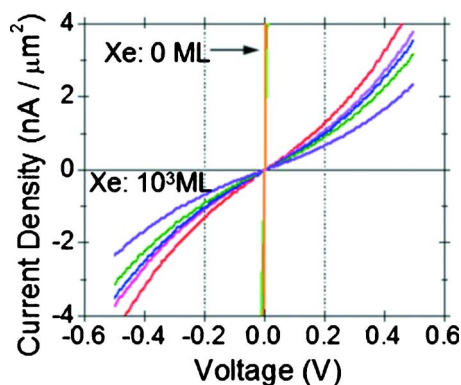


FIG. 4. (Color online) Randomly sampled, representative I-V characteristics of spots on a  $\sim 50 \mu\text{m}^2$  Au/C12-SAM/Au molecular junction prepared by the deposition of  $1180 \text{ atoms nm}^{-2}$  (256 atoms molecule<sup>-1</sup>) with a Xe buffer layer (1000 ML) and without Xe buffer layer (0 ML) at  $\sim 10 \text{ K}$ .

considerable sheet resistance arising from the low thickness, cluster morphology films. In contrast, devices prepared without a buffer layer exhibit short circuit points [Figs. 2(c) and 3(a)] with the expected Ohmic characteristics of Au metal filaments (data not shown).

The present results clearly demonstrate that the use of inert buffer layers can be used to control the quality of vapor deposited metal/molecule device junctions with the ability to eliminate troublesome artifacts such as short circuit metal filaments, thus allowing the fabrication of high integrity, large area metal/organic junctions. Further work is in progress to extend this processing method to the fabrication of large area devices with various types of molecules capable of such effects as bistable conduction states and to different types of deposited metals including highly reactive ones such as Ti and Ca.

The authors acknowledge funding from ONR, DTRA, and the PSU Center for Nanoscale Science (Grant No. MR-SEC DMR-0080019); the use of the PSU NSF NNIN site (Grant No. ECS-0335765); and the assistance of Pamela Long and Xuema Li (HP Laboratories) for sample preparations.

- <sup>1</sup>B. A. Mantoosh and P. S. Weiss, *Proc. IEEE* **9**, 1785 (2003).
- <sup>2</sup>J. C. Scott, *J. Vac. Sci. Technol. A* **21**, 521 (2003).
- <sup>3</sup>D. R. Jung and A. W. Czander, *Crit. Rev. Solid State Mater. Sci.* **19**, 1 (1994).
- <sup>4</sup>F. Faupel, R. Willecke, and A. Thran, *Mater. Sci. Eng. R.* **22**, 1 (1998).
- <sup>5</sup>N. J. Watkins, L. Yan, and Y. Gao, *Appl. Phys. Lett.* **80**, 4384 (2002).
- <sup>6</sup>R. L. Opila and J. Eng, Jr., *Prog. Surf. Sci.* **69**, 125 (2002).
- <sup>7</sup>A. Hooper, G. L. Fisher, K. Konstadinidis, D. Jung, H. Nguyen, R. Opila, R. W. Collins, N. Winograd, and D. L. Allara, *J. Am. Chem. Soc.* **121**, 8052 (1999).
- <sup>8</sup>Z. Zhu, T. A. Daniel, M. Maitani, O. M. Cabarcos, D. L. Allara, and N. Winograd, *J. Am. Chem. Soc.* **128**, 13710 (2006).
- <sup>9</sup>T. A. Daniel, Ph.D. thesis, Pennsylvania State University, 2005.
- <sup>10</sup>M. M. Maitani, T. A. Daniel, O. M. Cabarcos, and D. L. Allara, *J. Am. Chem. Soc.* **131**, 8016 (2009).
- <sup>11</sup>T. Ohgi, H.-Y. Sheng, and H. Nejo, *Appl. Surf. Sci.* **130-132**, 919 (1998).
- <sup>12</sup>D. R. Stewart, D. A. A. Ohlberg, P. A. Beck, Y. Chen, R. S. Williams, J. O. Jeppesen, K. A. Nielsen, and J. F. Stoddart, *Nano Lett.* **4**, 133 (2004).
- <sup>13</sup>W. Wang, T. Lee, and M. A. Reed, *Proc. IEEE* **93**, 1815 (2005).
- <sup>14</sup>H. Haick, O. Naitsoo, J. Ghabboun, and D. Cahen, *J. Phys. Chem. C* **111**, 2318 (2007).
- <sup>15</sup>H. B. Akkerman, P. W. M. Blom, D. M. de Leeuw, and B. de Boer, *Nature (London)* **441**, 69 (2006).
- <sup>16</sup>T. Xu, I. R. Peterson, M. V. Lakshmikantham, and R. M. Metzger, *Angew. Chem. Int. Ed.* **40**, 1749 (2001).
- <sup>17</sup>C. Haley and J. H. Weaver, *Surf. Sci.* **518**, 243 (2002).
- <sup>18</sup>G. D. Waddill, I. M. Vitomirov, C. M. Aldao, and J. H. Weaver, *Phys. Rev. Lett.* **62**, 1568 (1989).
- <sup>19</sup>R. Bhatia and B. J. Garrison, *Langmuir* **13**, 765 (1997).
- <sup>20</sup>S. Lee, S. S. Bae, G. Medeiros-Ribeiro, J. J. Blackstock, S. Kim, D. R. Stewart, and R. Ragan, *Langmuir* **24**, 5984 (2008).
- <sup>21</sup>R. G. Nuzzo, L. H. Dubois, and D. L. Allara, *J. Am. Chem. Soc.* **112**, 558 (1990).
- <sup>22</sup>C. D. Bain, E. B. Troughton, Y. T. Tao, J. Evall, G. M. Whitesides, and R. G. Nuzzo, *J. Am. Chem. Soc.* **111**, 321 (1989).
- <sup>23</sup>A. Salomon, D. Cahen, S. Lindsay, J. Tomfohr, V. B. Engelkes, and C. D. Frisbie, *Adv. Mater.* **15**, 1881 (2003).
- <sup>24</sup>M. M. Maitani, D. A. A. Ohlberg, Z. Li, D. L. Allara, D. R. Stewart, and R. S. Williams, *J. Am. Chem. Soc.* **131**, 6310 (2009).
- <sup>25</sup>See supplementary material at <http://dx.doi.org/10.1063/1.3377044> for AFM and TEM images of low coverage Au deposition samples.